JOURNAL OF AGRICULTURAL AND FOOD CHEMISTRY

Article

pubs.acs.org/JAFC

Color Quantification of Stained Maize Stem Section Describes Lignin Spatial Distribution within the Whole Stem

Yu Zhang,[†] Sylvain Legay,[†] Yves Barrière,[‡] Valérie Méchin,[†] and David Legland*[,§,#]

[†]Institut Jean-Pierre Bourgin, UMR 1318 INRA-AgroParisTech, INRA Centre de Versailles-Grignon, Route de Saint-Cyr, 78026 Versailles, France

[‡]INRA, UGAPF UR889, Unité de Génétique et d'Amélioration des Plantes Fourragères, B.P. 80006, 86600 Lusignan, France

[§]INRA, UMR782 Génie et Microbiologie des Procédés Alimentaires, 78850 Thiverval-Grignon, France

[#]AgroParisTech, UMR782 Génie et Microbiologie des Procédés Alimentaires, 78850 Thiverval-Grignon, France

ABSTRACT: This work presents a method to quantify the lignification of maize tissues by automated color image analysis of stained maize stem cross sections. Safranin and Alcian blue staining makes lignified tissues appear red, and nonlignified tissues appear blue. Lignification is assessed by the ratio of red intensity over blue intensity. A rough quantification of global lignification is computed as the surface ratio of lignified tissues. A more precise quantification is obtained by computing profiles of red/blue intensity ratio in relation to the distance to the epidermis, depicting the spatial distribution of lignified walls within the stem. Lignification profiles are analyzed through summary parameters describing the evolution of lignification in three specific regions. The distribution of lignification can be quickly assessed depending on the position and the development stage, allowing the screening of genetic variations to be envisioned.

KEYWORDS: *lignin distribution, internode development, stained stem cross section, image analysis, color quantification*

INTRODUCTION

Strong worldwide demand for energy and concern over global climate change have led to a resurgence in the development of alternative energy to replace fossil fuel for transportation. In response, many countries have initiated extensive research in this area. Cellulose, the "green gold", is of considerable nutritional and industrial importance and is the major substrate for the production of second-generation biofuels. Much of this cellulose is located in lignified secondary walls (lignocellulosics) in agricultural residues. To make these biofuels based on lignocellulosic agricultural residues effective, it is essential to identify the factors that induce lignocellulosic biomass recalcitrance in the presence of lignin and other phenolic compounds in secondary cell walls.

Plant cell walls are complex molecular assemblies that include polysaccharides (cellulose and hemicelluloses) and phenolic components (lignin and *p*-hydroxycinnamic acids). Lignin association with other cell wall constituents greatly modifies cell wall properties, including enzymatic degradability of structural polysaccharides.[1] Although it is clear that lignin has a negative impact on plant cell wall degradability, lignin content does not always appear to be a major factor in controlling degradability[2] and can only partially explain grass cell wall degradability variations.[3] Moreover, the pattern of lignification within the stem could lead to very different degradability profiles, thus highlighting the importance of anatomical structure and, more importantly, lignin distribution within the different stem tissues on grass cell wall degradability.[4,5] It has been suggested that anatomical structure might be more important than wall chemistry in determining the rate and extent of cell wall degradability.[6] Differences in anatomical structures for different tissues have been shown to widely influence accessibility to potentially degradable polysaccharides by rumen microorganisms.[6−8] Several studies have demonstrated that assessment of lignin distribution in stem tissues is necessary to evaluate its impact on grass cell wall degradability and thus to better optimize cell wall polysaccharides accessibility.[5,9−12]

Various techniques have been developed for the investigation of lignin distribution in tissues. Tissues can be physically dissected, either manually or by using laser capture microdissection.[13−15] Microdissection approaches are often combined with microbiochemical characterization.[13,15,16] However, these microdissections entail very tedious work[10,17,18] and are limited to the a priori choice of specific tissues. A powerful approach is to use microspectroscopy techniques, such as confocal fluorescence[19,20] or Raman[20−22] microscopy techniques. Although these methods provide very rich information, the observed field of view is usually small compared to the size of the stem. Consequently, the quantitative integration of many observations is usually done by focusing on a reduced number of specific cell types or tissues.

Histological stains are an alternative that can reveal specific components on a thin stem cross section with a minimum of preparation. Cell wall components react with the stain and become colored, revealing their distribution within the whole section. In a previous study, Méchin et al.[11] compared the use of Mäule,[23] phloroglucinol,[24] and Fasga[25] staining to assess the lignification of maize stem cross sections. Fasga staining, which

Received: November 13, 2012
Revised: March 7, 2013
Accepted: March 7, 2013
Published: March 7, 2013

makes lignified cell walls appear red and nonlignified lignified cell walls appear blue, was shown to be the most effective method. Even though red Safranin stain has been reported not to be strictly specific to lignins,[26,27] this staining appeared to be perfectly suitable for lignification studies.

In previous studies, lignification was quantified by the area ratio of lignified tissues.[11] However, global lignification can vary both with the lignification degree of cell wall in specific tissues and with the proportion of the different tissues within the stem cross section. Thus, the aim of this work was to develop a more precise method that also quantifies both the relative differences in lignification of different tissues and the spatial distribution of lignin in the whole cross section. The approach proposed in this study consists of the use of color as a quantitative measure that will be related to lignification. The subsequent color variations will thus make it possible to quantify the global lignification of single sections as well as the lignin distribution through profiles ranging from the epidermis to the center.

MATERIALS AND METHODS

Plant Material. The work presented in this paper was performed on stem cross sections of maize harvested at six developmental stages to cover a large range of variation for lignin distribution. The maize inbred line F324 was grown at the INRA Lusignan Centre (France) during the summer of 2011. Plots consisted of one 5.2 m long row with a density of 90000 plants per hectare. Irrigation was applied from mid-June to the end of August to prevent water stress. Principal ear internodes were sampled at six developmental stages beginning when the plants had reached the V8 (8 expanded leaves) stage. The next five stages were V10 (10 expanded leaves), tasseling, silking, 14 days after silking, and silage. Silage stage is attained when the dry matter content reaches 30%. In practice, this stage corresponds to the transition between a "milky grain" and "pasty grain". Five whole internodes (without the nodes) per developmental stage were sampled and immediately placed in 70% ethanol/water (v/v) for further histological analysis.

Image Acquisition. A 1 cm long segment was sampled in the middle part of each internode and soaked in water for 1 night. For each segment, 15 serial stem cross sections, 150 μm thick, were prepared with a vibratome (Leica VT1000 S).

Sections were stained overnight using a Safranin and Alcian blue solution. As previously reported,[25] Alcian blue may be used as a blue stain for cellulose and is compatible with Safranin O, which colors lignin in red. The staining solution was prepared as described[25] and composed of 11 mL of Alcian blue (0.2% in ethanol), 3 mL of Safranin O (0.1% in water), 1 mL of acetic acid, 30 mL of glycerin, and 20 mL of distilled water. After staining, sections were rinsed twice for 5 min with distilled water. Sections were examined under a magnifying glass (×1, Nikon SMZ 1000) and were digitized as color images by a ProgRes C3 digital microscope camera. The resolution was 10 μm per pixel. Color was represented by the three red, green, and blue channels, each of them being coded between 0 and 255. Lignified tissues were thus stained in red, whereas nonlignified or poorly lignified tissues appeared blue. Images acquired for the six development stages are presented in Figure 1.

Color Normalization. Because variations of the background light intensity were observed, a normalization procedure was applied to remove heterogeneity within and between images. The region of interest corresponding to the stem was segmented by applying Otsu's threshold on the green channel (Figure 2B), and the background image was extracted (Figure 2C). For each channel of the background image, a polynomial model depending on pixel coordinates was fitted from background values, resulting in an estimated background model for each image (Figure 2D). Normalized images were computed as the ratio of image over the corresponding background estimate (Figure 2E).

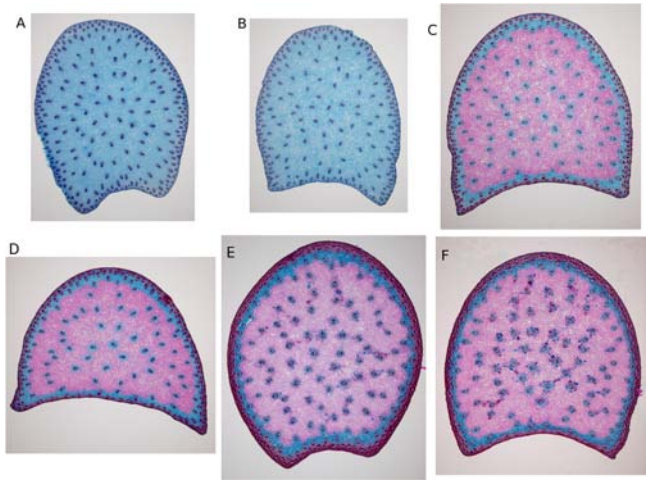

Figure 1. Image acquired (×1) after staining of 150 μm slices for each development stage: (A) 8 expanded leaves; (B) 10 expanded leaves; (C) tasseling; (D) silking; (E) 14 days after silking; (F) silage stage.

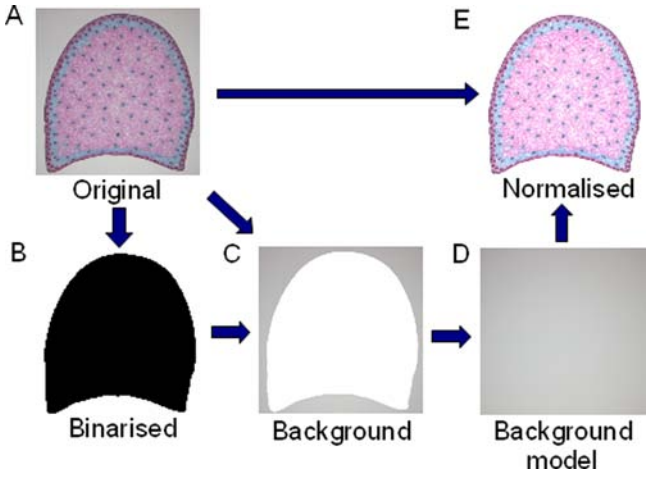

Figure 2. Normalization of color images using background model: (A) original image, sampled 14 days after silking; (B) region of interest; (C) background image; (D) estimated background model; (E) normalized images.

Proportion of Lignified Area. The lignification of the whole stem was assessed from normalized color images through the area fraction of lignified tissues. Because the staining did not color the interior of the cells, the coloration presented large variability, even in homogeneously stained tissues. A morphological opening was applied on each channel of the normalized color image.[28] All of the pixels of a given cell were associated with the color of its neighborhood, resulting in an image with homogeneous colored regions (Figure 3B).

The red, green, and blue channels of each image were separated (Figures 3C–E). The ratios of normalized red values over normalized blue values were used to assess the lignification corresponding to each pixel in the image (Figure 3F). The green channel was used to determine the region in the image corresponding to the parenchyma (Figure 3G). By applying a threshold to the ratio of red and blue intensities and combining it with that of the parenchyma region, it was possible to identify the lignified regions within the parenchyma (Figure 3H). The stem section was therefore classified into two regions: lignified and nonlignified. The ratio of lignified area over total parenchyma area was used as the index of global lignification.

Profile Computation. The quantification of lignification spatial distribution is more complicated because the cross sections present various shape and sizes. It is therefore necessary to consider a reference space that is common to all images. In the case of plant

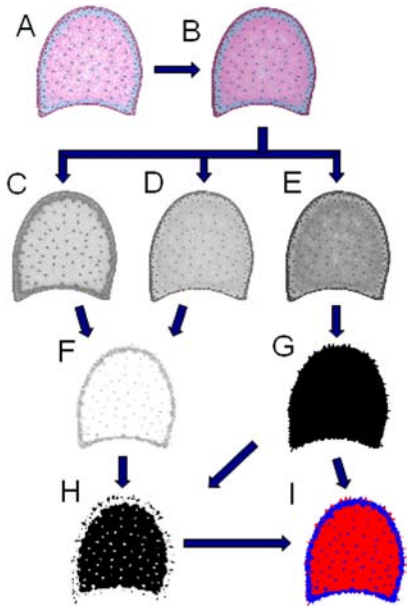

Figure 3. Computation of the proportion of lignified surface on a sample-normalized image sampled 14 days after silking: (A) original image; (B) morphological filtering; (C, D, E) red, blue, nd green channels of filtered image, respectively; (F) local red/blue ratio; (G) segmentation of parenchyma; (H) segmentation of lignified tissues; (I) classification of stem section into lignified and nonlignified regions.

organs, variations of cellular morphology can be assessed as a function of the relative distance to the epidermis.[29−31] Similarly, variations of lignification within the stem section were investigated in relation to the distance to the epidermis.

A distance map was computed for each pixel within the stem section (Figure 4), measuring an approximation of the Euclidean distance to

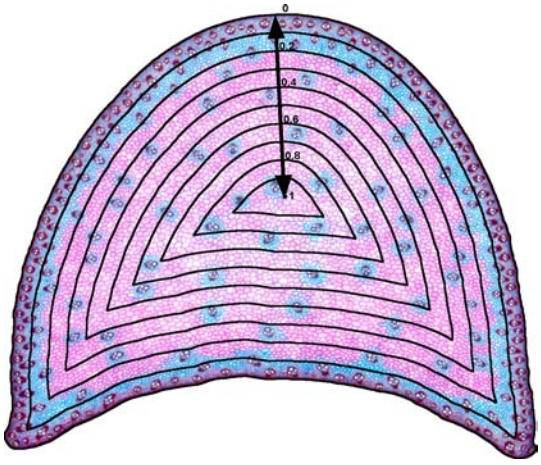

Figure 4. Partition of a stem section into a fixed number of regions. Ten regions are represented in this example. The image corresponds to a stem sampled 14 days after silking. Relative distances to epidermis are indicated.

the nearest background pixel. This distance map was divided into several concentric regions, corresponding to different classes of distances. A normalized distance was chosen: each stem section was divided into the same number of regions, and each region in a given image had the same breadth. A total of 80 regions with equal relative widths were chosen for all sections. Figure 4 shows an example of such a division, using only 10 regions for simplifying the visualization. Because the sizes of the sections vary, the breadths of the regions do not refer to the same physical breadth.

The red and blue intensity profiles relative to the distance to the epidermis (Figure 5A) were obtained by image analysis of the stained

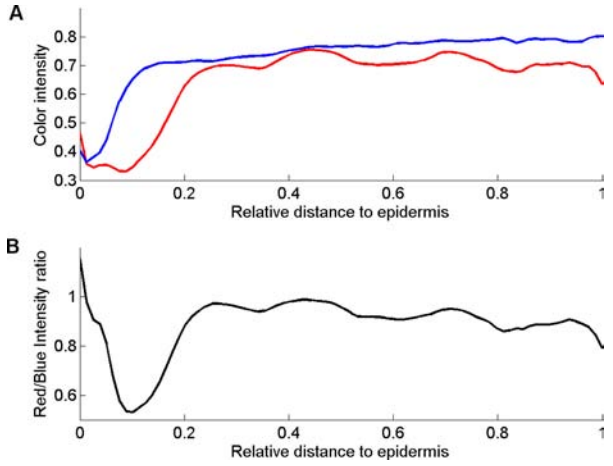

Figure 5. Intensity profiles measured according to the relative distance to the epidermis: (A) profiles of the blue and red intensities; (B) profile of the red/blue intensity ratio.

cross section. These profiles corresponded to the distribution within the section of tissues with lignified cell wall (red intensity) and of tissues with nonlignified cell walls (blue intensity). Because it was difficult to automatically recognize the locations of vascular bundles and sclerenchyma, no distinction was made between the different types of tissues. The blue profile of the sample image was lower for distances close to the epidermis than in the middle of the cross section. The red profile started to increase at a relative distance to the epidermis that was greater than that of the blue profile. The differences between the two profiles corresponded to the blue ring visible in Figure 4, exhibiting a region of the cortical parenchyma having cell walls that were not lignified. Some fluctuations could be observed in the red profile. They were interpreted as the influence of vascular bundles, which were surrounded by cells with nonlignified cell wall. The lignification profile was assessed by computing the ratio of the red intensity profile over that of the blue intensity profile (Figure 5B).

Statistical Analyses. Statistical analyses were performed within the Matlab environment (The Mathworks, Natick, MA, USA). Comparisons of group means were made using nonparametric Mann−Whitney−Wilcoxon tests, using a p value of 0.05 as the limit value.

RESULTS AND DISCUSSION

Proportion of Lignified Area. Red and blue areas could be discriminated by automatic image analysis of the section. This discrimination was used as a rough measure for the proportion of lignified tissues within the stem. In a previous study,[11] the accuracy of the Safranin and Alcian blue staining to study lignification of maize stem sections was established. In this study, the proportion of lignified area is measured over the whole stem section, thus providing theoretically more precise results, and is studied over several development stages (Figure 6).

The first two young developmental stages (V8 and V10) were poorly lignified, as expected. Only several small regions were lignified, mainly in the epidermis or inside vascular bundles. The proportion of lignified area subsequently increased to 70% at tasseling stage and gradually increased to 76% between the tasseling and silage stages. The lignified tissues were constituted quite exclusively of parenchyma. Large

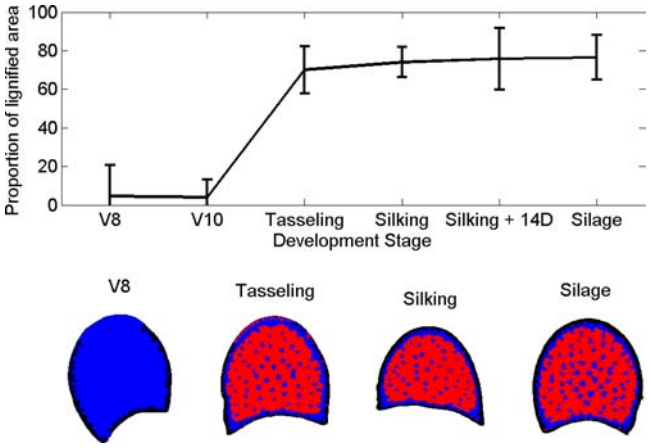

Figure 6. Evolution of the proportion of lignified area in stained sections during internode development, at the V8, V10, tasseling, silking, 14 days after silking, and silage stages.

regions of nonlignified parenchyma could be observed around vascular bundles. Vascular bundles of the parenchyma appeared as small lignified regions surrounded by nonlignified tissues.

The global increase of lignified area was in agreement with visual observations of stained stem sections. Lignified regions corresponded to those observed.[11] The automated discrimination of lignified tissues was found to adequately describe stem lignification during development. However, it was difficult to recognize the shape of vascular bundles from the resulting images. It was therefore assumed that the quantitative measurement of lignification at the pixel scale should describe more precisely the lignification process.

Profile of Lignification. The average profiles of the red/blue intensity ratio for each developmental stage are presented in Figure 7. The evolution of this ratio reflects the variations of lignification within stem sections from the epidermis to the center of the stem section.

The first two stages of development (V8 and V10) revealed homogeneous profiles with a relatively low value of the red/blue intensity ratio, corresponding to low global lignin content. In contrast, lignification profiles for the last four developmental stages (from tasseling to silage) presented higher values and large variations within the cross section.

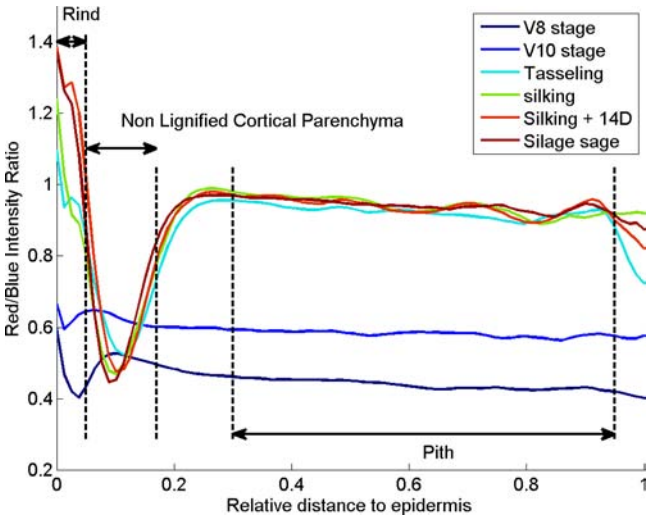

Figure 7. Average profiles of the red/blue intensity ratio relative to the distance to the epidermis for six stages of development. Specific regions of the stem cross section are indicated.

The V10 stage seemed to present a small increase of lignification (intensity ratio ~ 0.6) within the whole section compared to the V8 stage (intensity ratio ~ 0.45). However, no significant difference could be shown (p value of a Wilcoxon test = 0.39). For the last four development stages, global lignification was greater (p value < 1×10^{-3} for the difference between V10 and tasseling stages, and no significant differences between the last consecutive stages). The variation of lignification through the distance to the epidermis followed a quite similar pattern for the last four stages, and three concentric regions could be distinguished. A first region was characterized by a high red/blue intensity ratio for small relative distances to the epidermis. This region corresponded to epidermis and to subepidermis cells with lignified cell walls and will subsequently be referred to as rind.[5] Another region appeared as a blue ring on images and corresponded to cortical parenchyma with nonlignified cell walls. The third region of interest was the pith, which could be associated with a relative distance to the epidermis of >0.25.

Maximum values and differences between the stages were found in the rind region (relative distance range = 0−0.04). The red/blue intensity ratio in the rind increased during the internode development from 1.1 at tasseling stage to 1.4 at silage stage and made it possible to discriminate stages tasseling and silking from 14 days after silking and silage stages. Old stages presented an intense lignification in the rind region, whereas mid stages presented intermediate lignification in the rind region that was comparable with lignification in the pith region. The lowest values of the red/blue intensity ratio were observed in the region that corresponded to nonlignified cortical parenchyma (Figure 1). No significant variation was observed for the red/blue intensity ratio in either the nonlignified cortical parenchyma or the pith region over tasseling to silage stages. It could be hypothesized that the nonlignified cortical parenchyma disappeared over time while lignification occurred. However, this lignin-free region remained present while the intensification of lignification occurred in the rind region alone. In the same way, it was found that the parenchyma tissues were more degradable in this region than in the pith.[4] These results confirmed the very low lignification of the pith.

A great increase in the red/blue intensity ratio in the rind and pith regions between V10 and tasseling stages (p values < 1×10^{-3} for both regions) could be related to the lignification process of these regions. In the rind region, relatively high values of the red/blue intensity ratio indicated that cells from this region were much more lignified than those of other regions. Lignin content in this region increased until the last stage of development. The pith region presented lower lignification than the rind. Moreover, no significant variation of the lignification was apparent in the pith region for the last four stages.

Lignification Kinetics of Specific Stem Regions. The comparison of profiles can be simplified if they can be reduced to just a few summary parameters. Following the results presented above, four parameters are proposed. The first parameter is the lignification of the rind region, computed as the average value of the red/blue intensity ratio measured in the range of 0−0.04 of the relative distance to the epidermis. The second parameter is the lignification of the pith region,

computed as the average value of the red/blue intensity ratio measured in the range of 0.25−0.95.

For the developmental stages between tasseling and silage, a region corresponding to nonlignified cortical parenchyma could be distinguished. The position of this region was assessed from individual profiles by computing the set of contiguous regions close to the epidermis for which the lignification rate was <0.8. The nonlignified cortical parenchyma region was quantified by the average value of the red/blue intensity ratio and by the relative width of the region.

Figure 8 shows the evolution of the lignification for the three stem regions during internode development. The lignification

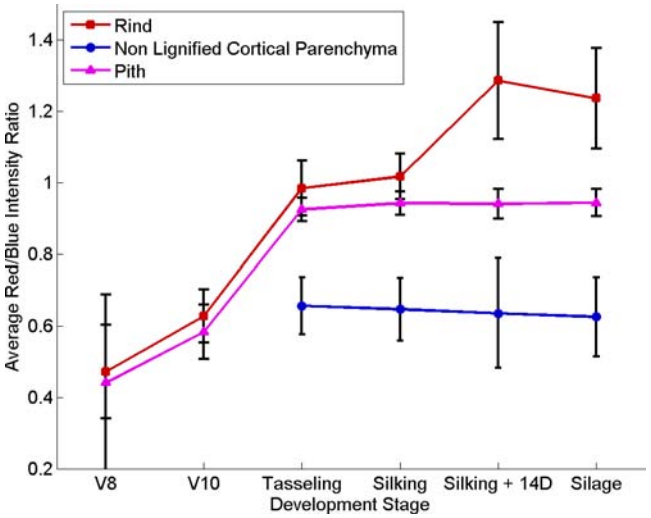

Figure 8. Evolution of the lignification for each region (rind, pith, nonlignified cortical parenchyma) of the stem sections during internode development.

of the rind region progressively increased throughout the developmental stages, starting from 0.47 ± 0.13, reaching a plateau around 1 at tasseling and silking stages, and further increasing at the later stages with a maximum value of 1.29 ± 0.16 at stage 14 days after silking.

The lignification of the pith showed a similar pattern for early development stages. Values increased from 0.44 ± 0.25 at stage V8 stage to 0.92 ± 0.03 at tasseling stage. For later developmental stages, lignification reached a plateau with a value of 0.94 ± 0.04 at silage stage.

Lignin deposition rates in the rind and pith regions were identical up to tasseling stage and then became differential. In grass, cell wall development shifts to a rapid deposition of lignified secondary wall development after the end of internode elongation.[4] In this study, the end of internode elongation corresponded to the tasseling stage. After cessation of internode elongation, the rind region developed an extensively lignified secondary wall, which is revealed by the gradual increase of lignification until the last stage. This lignification of a secondary wall does not seem to occur in the pith region, where no significant increase of lignin content was measured beyond tasseling stage.

The lignification of the nonlignified cortical parenchyma region was low (0.66 ± 0.08). No evolution of this parameter was found during internode development after tasseling stage. The relative width of this region was 0.14 ± 0.01 at tasseling stage. During internode development, no significant variation was observed for this parameter.

At the last stages of development (14 days after silking and silage stages), the three regions clearly presented strong differences in lignification. Differences of lignification between the rind and pith regions have been previously reported from chemical analyses of dissected tissues.[10] Further investigations showed that these differences were associated with variations of degradability because the tissues from the rind region are less degradable.[5,17,18] The parameters computed in this work are essential to better understand the regulation of plant degradation.

This work presents a method to quantify the lignification of maize tissues by using color image analysis of stained maize stem cross sections. Global lignification was assessed through the characterization of the proportion of the red area of each cross section. Lignification profiles within the stem were assessed by computing red/blue intensity ratio variations in relation to the distance to the epidermis. Variation profiles were analyzed by computing summary parameters describing the lignification of three specific stem regions: the epidermis, the blue ring, and the pith.

Lignification of maize internodes during development was thus explored in the major defined stem section regions. This level of observation is impossible to obtain with biochemical lignin content estimation except when using very tedious and complex microdissection approaches. The method developed in this paper makes it possible to easily and rapidly describe the lignification process during internode development. At young stages, lignification first occurs in the pith. After the silking stage, lignification becomes much more intense in the rind region. The parameters summarized from the red/blue intensity ratio profiles made it much easier to quantify the differences in lignification among stem regions. Results are in agreement with the biochemical analysis of dissected tissues in the literature. A great advantage of the proposed method is the possibility to quickly assess the distribution of lignin depending on the position in the section, without having to physically dissect the tissues. The image analysis procedure can be applied automatically to the whole image collection, requiring a few minutes for completion. The only limitation to the method is the time necessary to slice and stain the sections.

An interesting perspective would be to study the variation of lignification depending on the height in the plant, as well as the height in the internode. Several layers of nonlignified parenchyma cells were visible around vascular bundles in the pith on several images. These layers correspond to highly degradable regions.[5,20] It would therefore be of interest to quantify the profile of the lignification depending on the distance to the nearest vascular bundles. For that purpose, using high resolution and/or multispectral acquisition systems will greatly increase the quality of observations.[20] A potential difficulty for high-throughput image analysis would be the automatic identification of relevant tissues, such the bundles, or their boundary.

The lignification profiles were computed using the same reference space for all images. This gives the opportunity to quantitatively compare lignification on stems with various sizes or shapes. The whole methodology could also be extended to study lignification of other plant species, on the condition that lignin can also be stained adequately. The computation of the profiles requires the acquisition of images of the whole section and the identification of the reference structure, the epidermis in the case of this study.

The proposed method is generic and could be applied to analyze images obtained from alternative staining methods such as Mäule or phloroglucinol. The combination of several acquisition systems and/or staining can also be envisioned. It would be also of great interest to calibrate information obtained from image analysis with information obtained from local chemical analyses.

Further studies will focus on analyzing various maize lines to exhibit genotypic variations and the relationship between these histological parameters and cell wall degradability. The comparison of parameters obtained from color quantification will also be compared to parameters obtained at the microscopic scale, to link lignification to cell morphology. For example, it would be of interest to link the lignin content of cell walls to cell size or cell wall thickness. As the resolution increase usually causes a reduction of the field of view, it is expected that correlative microscopy techniques would be of interest to combine information obtained from microscopes operating at different scales.

The proposed method was a prerequisite for further studies devoted to the enhancement of cell wall degradability through cell wall improvement and to the elucidation of the genetic basis of lignin deposition and distribution all along the stem sections. The screening method presented here will make it possible to characterize a wide range of samples. The natural genetic variation for lignin distribution within the stem in relation to cell wall degradability will be the focus of future studies. We will also develop studies devoted to the genetic determinism of lignification both in the pith and in the rind regions. Work devoted to studying the genetic determinism of lignification will be undertaken, and the use of recombinant inbred line populations will undoubtedly shed light on the Quantitative Trait Loci (QTLs) steering these parameters.

AUTHOR INFORMATION

Corresponding Author

*E-mail: david.legland@grignon.inra.fr. Phone: +33 (0)130 815254. Fax: +33 (0)130 815597.

Funding

This work was funded by the French National Research Agency (ANR) in the context of the MAGIC program (ANR-08-BLAN-0307-01). Y.Z. was supported by a grant from INRA CEPIA and INRA BV.

Notes

The authors declare no competing financial interest.

ACKNOWLEDGMENTS

We sincerely acknowledge F. Legée and L. Cézard for their participation in lignin analysis, H. Morin for her assistance in histological analysis, and C. Minault, P. Vernoux, and D. Dénoue for their precious contribution to field experiments. The histological analyses were performed at the Plateforme de Cytologie et Imagerie Végétale (IJPB, Versailles).

REFERENCES

(1) Jung, H.; Samac, D.; Sarath, G. Modifying crops to increase cell wall digestibility. *Plant Sci.* **2012**, *185*, 65−77.

(2) Jung, H.; Buxton, D. Forage quality variation among maize inbreds: relationships of cell-wall composition and in-vitro degradability for stem internodes. *J. Sci. Food Agric.* **1994**, *66*, 313−322.

(3) Méchin, V.; Argillier, O.; Menanteau, V.; Barrière, Y.; Mila, I.; Pollet, B.; Lapierre, C. Relationship of cell wall composition to in vitro cell wall digestibility of maize inbred line stems. *J. Sci. Food Agric.* **2000**, *80*, 574−580.

(4) Jung, H.; Casler, M. Maize stem tissues: cell wall concentration and composition during development. *Crop Sci.* **2006**, *46*, 1793−1800.

(5) Jung, H.; Casler, M. Maize stem tissues: impact of development on cell wall degradability. *Crop Sci.* **2006**, *46*, 1801−1809.

(6) Wilson, J.; Mertens, D. Cell wall accessibility and cell structure limitations to microbial digestion of forage. *Crop Sci.* **1995**, *35*, 251−259.

(7) Wilson, J.; Hatfield, R. Structural and chemical changes of cell wall types during stem development: consequences for fibre degradation by rumen microflora. *Aust. J. Agric. Res.* **1997**, *48*, 165−180.

(8) Boon, E.; Struik, P.; Engels, F.; Cone, J. Stem characteristics of two forage maize (*Zea mays* L.) cultivars varying in whole plant digestibility. IV. Changes during the growing season in anatomy and chemical composition in relation to fermentation characteristics of a lower internode. *Neth. J. Agric. Sci.* **2012**, *59*, 13−23.

(9) Engels, F.; Schuurmans, J. Relationship between structural development of cell walls and degradation of tissues in maize stems. *J. Sci. Food Agric.* **1992**, *59*, 45−51.

(10) Wilson, J.; Mertens, D.; Hatfield, R. Isolates of cell types from sorghum stems: digestion, cell wall and anatomical characteristics. *J. Sci. Food Agric.* **1993**, *63*, 407−417.

(11) Méchin, V.; Argillier, O.; Rocher, F.; Hebert, Y.; Mila, I.; Pollet, B.; Barrière, Y.; Lapierre, C. In search of a maize ideotype for cell wall enzymatic degradability using histological and biochemical lignin characterization. *J. Agric. Food Chem.* **2005**, *53*, 5872−5881.

(12) Sarath, G.; Dien, B.; Saathoff, A.; Vogel, K.; Mitchell, R.; Chen, H. Ethanol yields and cell wall properties in divergently bred switchgrass genotypes. *Bioresour. Technol.* **2011**, *102*, 9579−9585.

(13) Chesson, A.; Provan, G.; Russell, W.; Scobbie, L.; Chabbert, B.; Monties, B. Characterisation of lignin from parenchyma and sclerenchyma cell walls of the maize internode. *J. Sci. Food Agric.* **1997**, *73*, 10−16.

(14) Angeles, G.; Berrio-Sierra, J.; Joseleau, J.; Lorimier, P.; Lefebvre, A.; Ruel, K. Preparative laser capture microdissection and single-pot cell wall material preparation: a novel method for tissue-specific analysis. *Planta* **2006**, *224*, 228−232.

(15) Ruel, K.; Berrio-Sierra, J.; Derikvand, M.; Pollet, B.; Thevenin, J.; Lapierre, C.; Jouanin, L.; Joseleau, J.-P. Impact of CCR1 silencing on the assembly of lignified secondary walls in *Arabidopsis thaliana*. *New Phytol.* **2009**, *184*, 99−113.

(16) Nakashima, J.; Chen, F.; Jackson, L.; Shadle, G.; Dixon, R. Multi-site genetic modification of monolignol biosynthesis in alfalfa (*Medicago sativa*): effects on lignin composition in specific cell types. *New Phytol.* **2008**, *179*, 1675−1685.

(17) Hatfield, R.; Wilson, J.; Mertens, D. Composition of cell walls isolated from cell types of grain sorghum stems. *J. Sci. Food Agric.* **1999**, *79*, 891−899.

(18) Barros-Rios, J.; Santiago, R.; Malvar, R. A.; Jung, H.-J. G. Chemical composition and cell wall polysaccharide degradability of pith and rind tissues from mature maize internodes. *Anim. Feed Sci. Technol.* **2012**, *172*, 226−236.

(19) Ma, J.; Yang, G.; Mao, J.; Xu, F. Characterization of anatomy, ultrastructure and lignin microdistribution in *Forsythia suspensa*. *Ind. Crops Prod.* **2011**, *33*, 358−363.

(20) Ding, L.-Y.; Liu, Y.-S.; Zeng, Y.; Himmel, M. E.; Baker, J. O.; Bayer, E. A. How does plant cell wall nanoscale architecture correlate with enzymatic digestibility? *Science* **2012**, *338*, 1055−1060.

(21) Chu, L.-Q.; Masyuko, R.; Sweedler, J. V.; Bohn, P. W. Base-induced delignification of *miscanthus* × *giganteus* studied by three-dimensional confocal raman imaging. *Bioresour. Technol.* **2010**, *101*, 4919−4925.

(22) Allouche, F.; Hanafi, M.; Jamme, F.; Robert, P.; Guillon, F.; Devaux, M. Coupling hyperspectral image data having different spatial resolutions by extending multivariate inter-battery Tucker analysis. *Chemom. Intell. Lab. Syst.* **2012**, *113*, 43−51.

(23) Browning, B. *Methods of Wood Chemistry*; Wiley: New York., 1967; Vol. *I* and *II*.
(24) Brauns, F. *The Chemistry of Lignin*; Academic Press: New York, 1952.
(25) Tolivia, D.; Tolivia, J. Fasga: a new polychromatic method for simultaneous and differential staining of plant tissues. *J. Microsc.* **1987**, *148*, 113−117.
(26) Johansen, D. *Plant Micro Technique*; McGraw-Hill: New York, 1940.
(27) Wilcox, W. *Preparation of Decayed Wood for Microscopic Examination*; U.S. Forestry Service Research Note FPL-056; 1964.
(28) Soille, P. *Morphological Image Analysis*; Springer-Verlag: Berlin, Germany, 2003.
(29) Ho, Q.; Verboven, P.; Verlinden, B.; Schenk, A.; Delele, M.; Rolletschek, H.; Vercammen, J.; Nicolaï, B. Genotype effects on internal gas gradients in apple fruit. *J. Exp. Bot.* **2010**, *61*, 2745−2755.
(30) Legland, D.; Guillon, F.; Kiêu, K.; Bouchet, B.; Devaux, M.-F. Stereological estimation of cell wall density of DR12 tomato mutant using three-dimensional confocal imaging. *Ann. Bot.* **2010**, *105*, 265−276.
(31) Legland, D.; Devaux, M.; Bouchet, B.; Guillon, F.; Lahaye, M. Cartography of cell morphology in tomato pericarp at the fruit scale. *J. Microsc.* **2012**, *247*, 78−93.